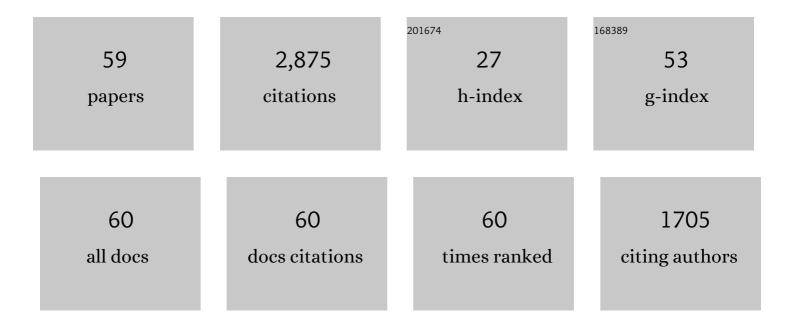
Sarah E Gilbert

List of Publications by Year in descending order

Source: https://exaly.com/author-pdf/8741205/publications.pdf Version: 2024-02-01



#	Article	IF	CITATIONS
1	Gold and Trace Element Zonation in Pyrite Using a Laser Imaging Technique: Implications for the Timing of Gold in Orogenic and Carlin-Style Sediment-Hosted Deposits. Economic Geology, 2009, 104, 635-668.	3.8	748
2	Routine quantitative multi-element analysis of sulphide minerals by laser ablation ICP-MS: Standard development and consideration of matrix effects. Geochemistry: Exploration, Environment, Analysis, 2011, 11, 51-60.	0.9	211
3	Age and pyrite Pb-isotopic composition of the giant Sukhoi Log sediment-hosted gold deposit, Russia. Geochimica Et Cosmochimica Acta, 2008, 72, 2377-2391.	3.9	151
4	Gold-telluride nanoparticles revealed in arsenic-free pyrite. American Mineralogist, 2012, 97, 1515-1518.	1.9	150
5	Minor and trace elements in bornite and associated Cu–(Fe)-sulfides: A LA-ICP-MS studyBornite mineral chemistry. Geochimica Et Cosmochimica Acta, 2011, 75, 6473-6496.	3.9	118
6	Optimisation of laser parameters for the analysis of sulphur isotopes in sulphide minerals by laser ablation ICP-MS. Journal of Analytical Atomic Spectrometry, 2014, 29, 1042-1051.	3.0	96
7	Multivariate Analysis of an LA-ICP-MS Trace Element Dataset for Pyrite. Mathematical Geosciences, 2012, 44, 823-842.	2.4	90
8	Development of Framboidal Pyrite During Diagenesis, Low-Grade Regional Metamorphism, and Hydrothermal Alteration. Economic Geology, 2009, 104, 1143-1168.	3.8	84
9	LA-ICPMS and EPMA studies of pyrite, arsenopyrite and loellingite from the Bhukia-Jagpura gold prospect, southern Rajasthan, India: Implications for ore genesis and gold remobilization. Chemical Geology, 2012, 326-327, 72-87.	3.3	80
10	In situ Pb-isotope analysis of pyrite by laser ablation (multi-collector and quadrupole) ICPMS. Chemical Geology, 2009, 262, 344-354.	3.3	74
11	Evidence for an Intrabasinal Source and Multiple Concentration Processes in the Formation of the Carbon Leader Reef, Witwatersrand Supergroup, South Africa. Economic Geology, 2013, 108, 1215-1241.	3.8	63
12	In-situ Lu Hf geochronology of garnet, apatite and xenotime by LA ICP MS/MS. Chemical Geology, 2021, 577, 120299.	3.3	62
13	Geometallurgy of the Pebble Porphyry Copper-Gold-Molybdenum Deposit, Alaska: Implications for Gold Distribution and Paragenesis. Economic Geology, 2013, 108, 463-482.	3.8	60
14	Textures and U-W-Sn-Mo signatures in hematite from the Olympic Dam Cu-U-Au-Ag deposit, South Australia: Defining the archetype for IOCG deposits. Ore Geology Reviews, 2017, 91, 173-195.	2.7	54
15	A Comparative Study of Five Reference Materials and the Lombard Meteorite for the Determination of the Platinumâ€Group Elements and Gold by LAâ€ICPâ€MS. Geostandards and Geoanalytical Research, 2013, 37, 51-64.	3.1	53
16	Indium distribution in sphalerite from sulfide–oxide–silicate skarn assemblages: a case study of the Dulong Zn–Sn–In deposit, Southwest China. Mineralium Deposita, 2021, 56, 307-324.	4.1	53
17	Fractionation of sulphur relative to iron during laser ablation-ICP-MS analyses of sulphide minerals: implications for quantification. Journal of Analytical Atomic Spectrometry, 2014, 29, 1024-1033.	3.0	46
18	Thermochronological and geochemical footprints of post-orogenic fluid alteration recorded in apatite: Implications for mineralisation in the Uzbek Tian Shan. Gondwana Research, 2019, 71, 1-15.	6.0	39

SARAH E GILBERT

#	Article	IF	CITATIONS
19	Evolution of a hydrothermal ore-forming system recorded by sulfide mineral chemistry: a case study from the Plaka Pb–Zn–Ag Deposit, Lavrion, Greece. Mineralium Deposita, 2022, 57, 417-438.	4.1	38
20	Assessment of elemental fractionation and matrix effects during <i>in situ</i> Rb–Sr dating of phlogopite by LA-ICP-MS/MS: implications for the accuracy and precision of mineral ages. Journal of Analytical Atomic Spectrometry, 2021, 36, 322-344.	3.0	37
21	A multi-technique evaluation of hydrothermal hematite U Pb isotope systematics: Implications for ore deposit geochronology. Chemical Geology, 2019, 513, 54-72.	3.3	36
22	LA–ICP–MS and EPMA studies on the Fe–S–As minerals from the Jinlongshan gold deposit, Qinling Orogen, China: implications for oreâ€forming processes. Geological Journal, 2014, 49, 482-500.	1.3	32
23	Hydrothermal and metamorphic fluid-rock interaction associated with hypogene "hard―iron ore mineralisation in the Quadrilátero FerrÃfero, Brazil: Implications from in-situ laser ablation ICP-MS iron oxide chemistry. Ore Geology Reviews, 2015, 69, 325-351.	2.7	32
24	Syn-tectonic sulphide remobilization and trace element redistribution at the Falun pyritic Zn-Pb-Cu-(Au-Ag) sulphide deposit, Bergslagen, Sweden. Ore Geology Reviews, 2018, 96, 48-71.	2.7	32
25	The effects of hardpan layers on the water chemistry from the leaching of pyrrhotite-rich tailings material. Environmental Geology, 2003, 44, 687-697.	1.2	30
26	Concentration of Particulate Platinum-Group Minerals during Magma Emplacement; a Case Study from the Merensky Reef, Bushveld Complex. Journal of Petrology, 2015, 56, 113-159.	2.8	29
27	Cu–Ni–PGE fertility of the Yoko-Dovyren layered massif (northern Transbaikalia, Russia): thermodynamic modeling of sulfide compositions in low mineralized dunite based on quantitative sulfide mineralogy. Mineralium Deposita, 2016, 51, 993-1011.	4.1	29
28	Rare Earth Element Fluorocarbonate Minerals from the Olympic Dam Cu-U-Au-Ag Deposit, South Australia. Minerals (Basel, Switzerland), 2017, 7, 202.	2.0	26
29	Textures and trace element composition of pyrite from the Bukit Botol volcanic-hosted massive sulphide deposit, Peninsular Malaysia. Journal of Asian Earth Sciences, 2018, 158, 173-185.	2.3	26
30	Halogens in hydrothermal sphalerite record origin of ore-forming fluids. Geology, 2020, 48, 766-770.	4.4	21
31	Structural evolution and medium-temperature thermochronology of central Madagascar: implications for Gondwana amalgamation. Journal of the Geological Society, 2020, 177, 784-798.	2.1	17
32	Rare Earth Element Phosphate Minerals from the Olympic Dam Cu-U-Au-Ag Deposit, South Australia: Recognizing Temporal-Spatial Controls On Ree Mineralogy in an Evolved IOCG System. Canadian Mineralogist, 2019, 57, 3-24.	1.0	15
33	Coupled U-Pb and Rb-Sr laser ablation geochronology trace Archean to Proterozoic crustal evolution in the Dharwar Craton, India. Precambrian Research, 2020, 343, 105709.	2.7	15
34	<i>In situ</i> laser ablation Lu–Hf geochronology of garnet across the Western Gneiss Region: campaign-style dating of metamorphism. Journal of the Geological Society, 2022, 179, .	2.1	15
35	Multivariate Statistical Analysis of Trace Elements in Pyrite: Prediction, Bias and Artefacts in Defining Mineral Signatures. Minerals (Basel, Switzerland), 2020, 10, 61.	2.0	14
36	Uptake of trace elements by baryte during copper ore processing: A case study from Olympic Dam, South Australia. Minerals Engineering, 2019, 135, 83-94.	4.3	13

SARAH E GILBERT

#	Article	IF	CITATIONS
37	Removal of Hg interferences for common Pb correction when dating apatite and titanite by LA-ICP-MS/MS. Journal of Analytical Atomic Spectrometry, 2020, 35, 1472-1481.	3.0	13
38	Unraveling the histories of Proterozoic shales through <i>in situ</i> Rb-Sr dating and trace element laser ablation analysis. Geology, 2022, 50, 66-70.	4.4	13
39	In situ Lu–Hf geochronology of calcite. Geochronology, 2022, 4, 353-372.	2.5	13
40	Iron-oxides constrain BIF evolution in terranes with protracted geological histories: The Iron Count prospect, Middleback Ranges, South Australia. Lithos, 2019, 324-325, 20-38.	1.4	12
41	Trace element distributions in (Cu)-Pb-Sb sulfosalts from the Gutaishan Au-Sb deposit, South China: Implications for formation of high fineness native gold. American Mineralogist, 2019, 104, 425-437.	1.9	11
42	Rapid, competitive radium uptake in strontium, barium, and lead sulfates during sulfuric acid leaching. Applied Geochemistry, 2020, 115, 104549.	3.0	11
43	Transgenerational marking of cephalopods with an enriched barium isotope: a promising tool for empirically estimating post-hatching movement and population connectivity. ICES Journal of Marine Science, 2010, 67, 1372-1380.	2.5	10
44	Matrix dependency for oxide production rates by LA-ICP-MS. Journal of Analytical Atomic Spectrometry, 2017, 32, 638-646.	3.0	10
45	Trace element substitution and grain-scale compositional heterogeneity in enargite. Ore Geology Reviews, 2019, 111, 103004.	2.7	10
46	A laser ablation technique maps differences in elemental composition in roots of two barley cultivars subjected to salinity stress. Plant Journal, 2020, 101, 1462-1473.	5.7	10
47	A simple and rapid ICP-MS/MS determination of sulfur isotope ratios (34S/32S) in complex natural waters: A new tool for tracing seawater intrusion in coastal systems. Talanta, 2021, 235, 122708.	5.5	10
48	Constraints from in-situ Rb-Sr dating on the timing of tectono-thermal events in the Umm Farwah shear zone and associated Cu-Au mineralisation in the Southern Arabian Shield, Saudi Arabia. Journal of Asian Earth Sciences, 2022, 224, 105037.	2.3	10
49	Laser-ablation Lu-Hf dating reveals Laurentian garnet in subducted rocks from southern Australia. Geology, 2022, 50, 837-842.	4.4	10
50	Effect of Selenium and Iodine on Oxidative Stress in the First Trimester Human Placenta Explants. Nutrients, 2021, 13, 800.	4.1	9
51	Detrital apatite <scp>Lu–Hf</scp> and <scp>U–Pb</scp> geochronology applied to the southwestern Siberian margin. Terra Nova, 2022, 34, 201-209.	2.1	9
52	Early Evolution of the Adelaide Superbasin. Geosciences (Switzerland), 2022, 12, 154.	2.2	5
53	Textural and geochemical analysis of celestine and sulfides constrain Sr-(Pb-Zn) mineralization in the Shizilishan deposit, eastern China. Ore Geology Reviews, 2022, 144, 104814.	2.7	5
54	Intermobility of barium, strontium, and lead in chloride and sulfate leach solutions. Geochemical Transactions, 2019, 20, 4.	0.7	3

#	Article	IF	CITATIONS
55	Synthesis of U-Pb doped hematite using a hydrated ferric oxide approach. Journal of Crystal Growth, 2019, 513, 48-57.	1.5	3
56	A Synthetic Haematite Reference Material for LAâ€ICPâ€MS Uâ€Pb Geochronology and Application to Iron Oxideâ€Cuâ€Au Systems. Geostandards and Geoanalytical Research, 2021, 45, 143-159.	3.1	3
57	Geochemistry of Sphalerite from the Permian Volcanic-Hosted Massive Sulphide (VHMS) Deposits in the Tasik Chini Area, Peninsular Malaysia: Constraints for Ore Genesis. Minerals (Basel, Switzerland), 2021, 11, 728.	2.0	3
58	In situ Lu–Hf phosphate geochronology: Progress towards a new tool for space exploration. Geoscience Frontiers, 2022, 13, 101375.	8.4	2
59	Development and Application of Synthetic Hematite Reference Material for U-Pb Geochronology. Microscopy and Microanalysis, 2021, 27, 2742-2745.	0.4	0